Supporting Information

Santagata et al. 10.1073/pnas.1404724111

Extended Description of Fig. 4*A*

Intraoperative MS allows for significant advances in the frequency of intraoperative tissue sampling as well as improvements in time from tissue sampling to availability of tissue analysis that can influence intraoperative surgical decision making. The schematic in Fig. 4*A* shows standard-of-care practices including pre- and postoperative tests (including preoperative planning MRI, permanent surgical tumor pathology analysis, and genomic analysis of intraoperative tumor tissue samples). Also demonstrated is the intraoperative (i.e., surgical) workflow, including intraoperative MRI, frozen sectioning, and MS tissue analysis. All intraoperative time periods are drawn to scale according to the time required for each test. Currently, on a research basis, intraoperative MS analysis is typically completed within 2 min, whereas frozen section analysis is completed in 20–30 min and intraoperative MRI requires at least 60 min. The time course of each intraoperative analytical measurement is measured from the time that the tissue sample is taken from the brain of the patient (or the time that the patient is readied for MRI scanning) until information from the test can returned to the surgeon to help guide the remainder of the surgery. The MS analysis time points denote an example of the timing and frequency of representative sampling periods during an operation. MS time periods (hash-marked orange rectangles) connote that MS is not yet standard of care and is a research test.

Tissue Samples

All samples were obtained and analyzed under Institutional Review Board protocols approved at Brigham and Women's Hospital (BWH) and Dana–Farber Cancer Institute. Informed written consent was obtained by neurosurgeons at BWH. Tumors were rereviewed and classified in accordance with the World Health Organization classification system by board-certified neuropathologists (S.S., K.L.L.). Resections of brain tumor lesions were performed using neuronavigation, with stereotactic mapping and spatial registering of biopsies performed. Three-dimensional reconstructions of the tumor from MRI imaging data were achieved with the 3D Slicer software package. Gliobastoma xenografts BT116 and BT329 were derived from surgical resection material acquired from patients undergoing neurosurgery at the BWH on an Institutional Review Board-approved protocol. Briefly, tumor resection samples were enzymatically and mechanically dissociated using the MACS Brain Tumor Dissociation Kit (Miltenyi Biotech) to generate single-cell suspensions. Intracranial xenografts were generated by injecting 100,000 cells in the right striatum of SCID mice (IcrTac:ICR-Prkdcscid; Charles River Labs) and aged under standard conditions until onset of neurological symptoms. Killed xenografts were perfused by intracardiac injection of 4% paraformaldehyde and processed by standard methods for paraffin embedding.

Histopathology and Immunohistochemistry. In addition to banked snap-frozen samples, all cases had tissue samples that were formalin-fixed and paraffin-embedded (FFPE). Sections of FFPE tissue were stained with an anti-isocitrate dehydrogenase 1 (IDH1)-R132H antibody (clone HMab-1 from EMD Millipore) as previously described. H&E-stained serial tissue sections were scanned using Mirax Micro 4SL telepathology system from Zeiss to generate digital optical images. Tumor content was evaluated by board-certified neuropathologists (S.S. and K.L.L.) through examination of H&E-stained tissue sections and IDH1 R132H-stained sections.

Identification of 2-Hydroxyglutarate by Desorption Electrospray Ionization MS. The IDH1 status of each specimen was initially evaluated by immunohistochemistry (IHC) of a piece of FFPE tissue. For stereotactic cases, all biopsies were less than 0.4 cm and these specimens were divided into two [one portion was frozen for desorption electrospray ionization (DESI) MS studies and the other was processed for FFPE; the latter was used for IDH1 IHC].

To determine whether 2-hydroxyglutarate (2-HG) could be detected directly from glioma tissue sections by DESI MS imaging, we analyzed human glioma samples by DESI MS in the negative ion mode using either a linear trap quadrupole (LTQ) ion trap (Thermo Fisher Scientific) or an amaZon speed ion trap (Bruker Daltonics). The solvent used in these experiments consisted of either MeOH:H_2O (1:1) or ACN:DMF (1:1) with a mass from *m/z* 100–1,100. All experiments involving the amaZon speed ion trap were carried out using a 5-kV spray voltage, 130 psi nebulizing gas (N_2), and a flow rate of 0.7 μL/min.

Tandem MS analysis was used for identification of the molecular species at *m/z* 147.2. Further characterization was performed by tandem MS with an additional stage of MS analysis (MS^3). The standard compound L-α-hydroxyglutaric acid disodium salt (Sigma-Aldrich Inc.) was subjected to tandem MS experiments under the same conditions. Confirmation experiments were performed using a high-resolution LTQ Orbitrap mass spectrometer (Thermo Fisher Scientific). Further analysis was then conducted with the amaZon speed ion trap. For this instrument, the 2-HG signal was located at *m/z* 146.9 and was assigned using a mouse brain that contained a large tumor with the 2-HG mutation. Tandem MS and MS^3 experiments were conducted on this peak to confirm its identity and found to be identical to the fragmentation pattern obtained with the LTQ instrument. Imaging of another mouse brain that had another tumor without the 2-HG mutation did not show this peak.

A description of the samples used in this initial testing stage of this study (analyzed with the LTQ ion trap) is shown in Table S1. Negative ion mode DESI MS mass spectra of samples G23 and G31 are shown in Fig. 1, using MeOH:H_2O (1:1) as the solvent system. In total, we analyzed 35 human glioma samples presented in Table S1, including oligodendrogliomas, astrocytomas, and oligoastrocytomas of different grades and varying tumor cell concentrations, using both ion trap mass spectrometers. Note that because tissue analysis by DESI MS is performed without sample preparation but directly on tissue section, standard quantification of 2-HG as commonly performed with time-consuming HPLC-MS protocols is not possible. One means by which relative levels of a certain molecule can be calculated is by normalizing its signal to a reference signal or set of signals obtained from the sample. In our study, the total abundance of 2-HG signal at *m/z* 147 was normalized to the sum of total abundances of the most abundant lipid species detected from the glioma samples by DESI MS. The mass spectra were exported as nominal mass from Xcalibur software (Thermo Fisher Scientific), and the absolute intensities of the 40 most abundant lipid species within *m/z* 700–1,000, which had been previously identified by tandem MS, were summed. Noise or background peaks within that *m/z* range were not considered. Normalization was then accomplished by dividing the total intensity of 147 by the summed intensities of the lipid species. Note that because

a small contribution of background signal at the same *m/z* 147 was present in DESI mass spectra, MS^2 was performed for all samples to confirm the presence of 2-HG. This was especially important in some *IDH1* mutant samples with low tumor cell concentrations and therefore much lower abundances of 2-HG in DESI mass spectrum. If the MS^2 fragmentation pattern matched that of authentic 2-HG, the sample was determined to be IDH1-mutated. Discrepancies in the fragmentation pattern or absence of detectable levels of *m/z* 147 were interpreted as IDH wild type by MS analysis. Results for DESI MS analysis were obtained using two solvent systems. Note that although the solvent system DMF:ACN (1:1) favored relative abundances of low *m/z* ions compared with MeOH:H_2O, similar trends in 2-HG were observed for both solvents. Interestingly, the ratio of *m/z* 147 to the sum of lipid species correlated with the tumor cell concentration determined for the sample by histopathological evaluation of serial tissue section, providing a direct measure of the 2-HG levels in tissue. Most samples that were negative for IDH1 mutation as determined by IHC did not present 2-HG in the DESI MS mass spectra, even if the sample presented high tumor cell concentration, as confirmed by tandem MS analysis (with the exception of two samples as noted in the text).

One of the challenges in the analysis was to determine IDH1 status by DESI MS detection of 2-HG in samples with low tumor cell concentration from full mass spectral data. For these samples, low detectable values of *m/z* 147 could be initially assumed as an indication of IDH negative mutation. Nevertheless, MS^2 and MS^3 of *m/z* 147 enabled IDH mutation status confirmation for these samples, despite the low tumor cell concentration (as low as ~5% of tumor). DESI MS imaging was performed for a few of the samples analyzed to evaluate the distribution of 2-HG and other diagnostic lipid species compared with tumor cell distribution in tissue.

Genetic Analysis

Archival surgical specimens were reviewed by a pathologist (S.S.) to select the most appropriate tumor-enriched area for analysis. Total nucleic acid was extracted from FFPE tumor tissue obtained by manual macrodissection, followed by extraction using a modified FormaPure System (Agencourt Bioscience Corporation). Targeted mutational analysis (SNaPshot) of a panel of cancer genes that included *IDH1* and *IDH2* was performed.

The primers listed below were used for targeted mutation analysis at codon R132 in *IDH1* (nucleotide positions c.394 and c.395) and at codons R140 and R172 in *IDH2* (nucleotide positions c.418, c.419, c.514 and c.515). PCR primers: *IDH1* exon 4, 5′-ACGTTGGATGGGCTTGTGAGTGGATGGGTA-3′ (forward) and 5′- ACGTTGGATGGCAAAATCACATTATTGCCAAC-3′ (reverse); *IDH2* exon 4a (to probe codon R140), 5′- ACGTTGGATGGCTGCAGTGGGACCACTATT-3′ (forward), and 5′- ACGTTGGATGTGGGATGTTTTTGCAGATGA-3′ (reverse); and *IDH2* exon 4b (to probe codon R172), 5′- ACGTTGGATGAACATCCCACGCCTAGTCC-3′ (forward), and 5′- ACGTTGGATGCAGTGGATCCCCTCTCCAC-3′ (reverse).

Extension primers: IDH1.394 extR 5′-GACTGACTGGACTGACTGACTGACTGACTGGACTGACTGACTGAGATCCCCATAAGCATGAC-3′, IDH1.395 extR 5′-TGATCCCCATAAGCATGA-3′, IDH2.418 extR 5′-GACTGACTGACTGACTGACTGACTGACTGACTGGACTGACTGACTGACTGCCCCCAGGATGTTCC-3′, IDH2.419 extF 5′-GACTGACTGGACTGACTGACTGACTGAGTCCCAATGGAACTATCC-3′, IDH2.514 extF 5′-GACTGACTGACTGACTGACTGACTGACTGACTGGACTGACTGACTGACTGACTGGACTGACTGACCCATCACCATTGGC-3′, and IDH2.515 extR 5′- GACTGACTGACTGACTGACTGACTGACTGACTGACTGGACTGACTGACTGACTGACTGGACTGACTGAGCCATGGGCGTGC-3′.

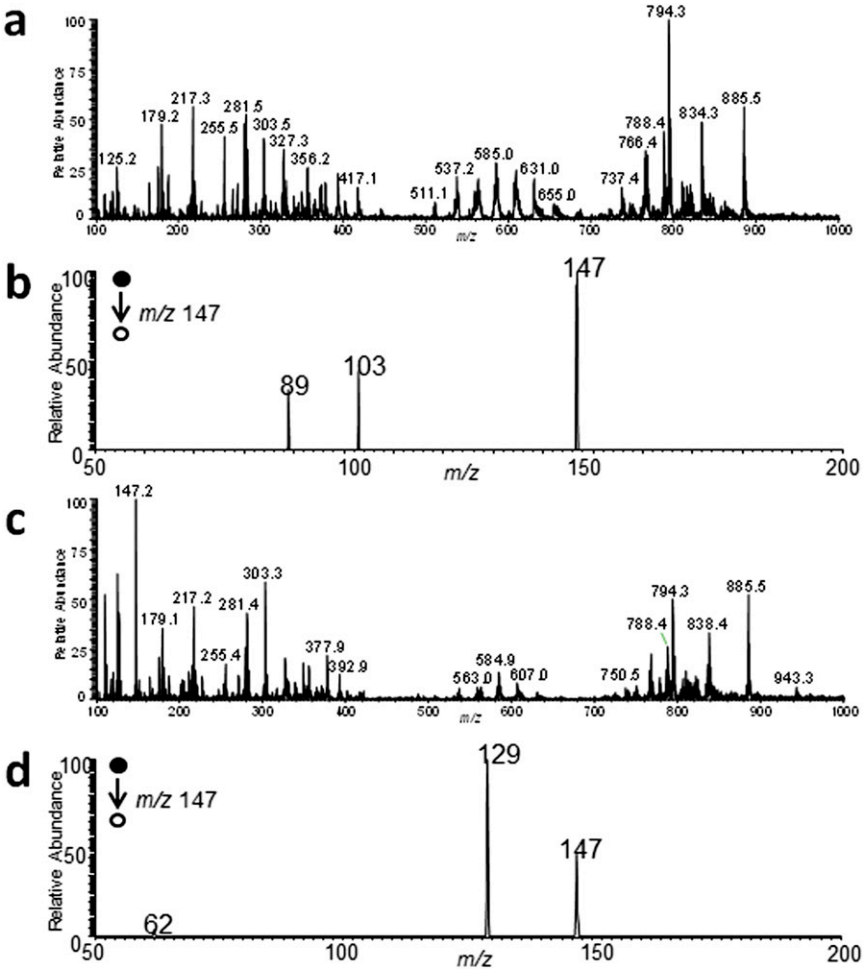

Fig. S1. Negative ion mode DESI mass spectrum from *m/z* 100–1,000 of (*A*) sample G31, a glioblastoma with wild-type IDH1. (*B*) Tandem mass spectrum of a low abundance ion detected at *m/z* 147 from sample G31 presents a fragmentation pattern that does not match that of standard 2-HG. Negative ion mode DESI mass spectrum from *m/z* 100–1,000 of (*C*) sample G23, an oligodendroglioma with the IDH1 R132H mutant shows high abundance of an ion at *m/z* 147.2. (*D*) Tandem mass spectrum of *m/z* 147.2 detected from sample G23 presents a fragmentation pattern that exactly matches that of standard 2-HG.

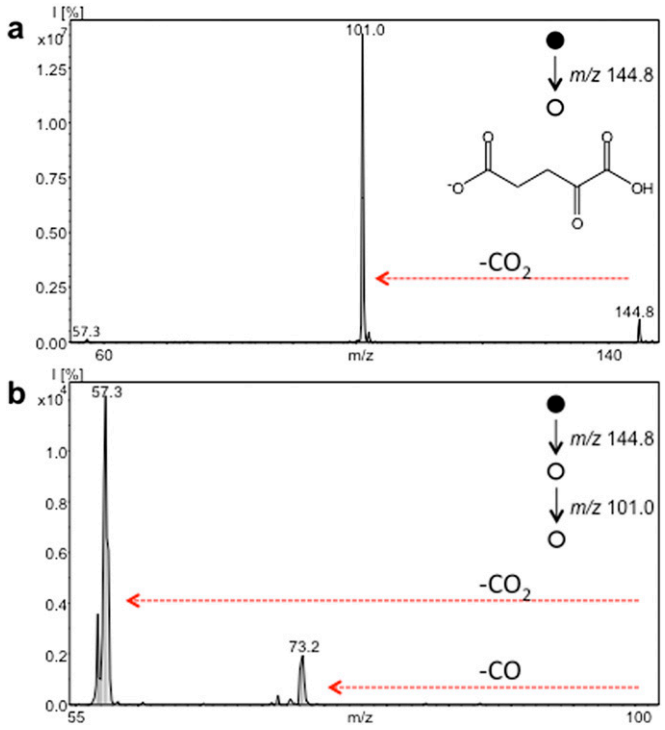

Fig. S2. Tandem mass spectra obtained from an α-ketoglutaric acid standard solution (*m/z* 144.8) in negative ion mode electrospray ionization using an amaZon Speed ion trap [MS^2 of *m/z* 144.8 (*A*); MS^3 of the fragment *m/z* 101.0 (*B*)].

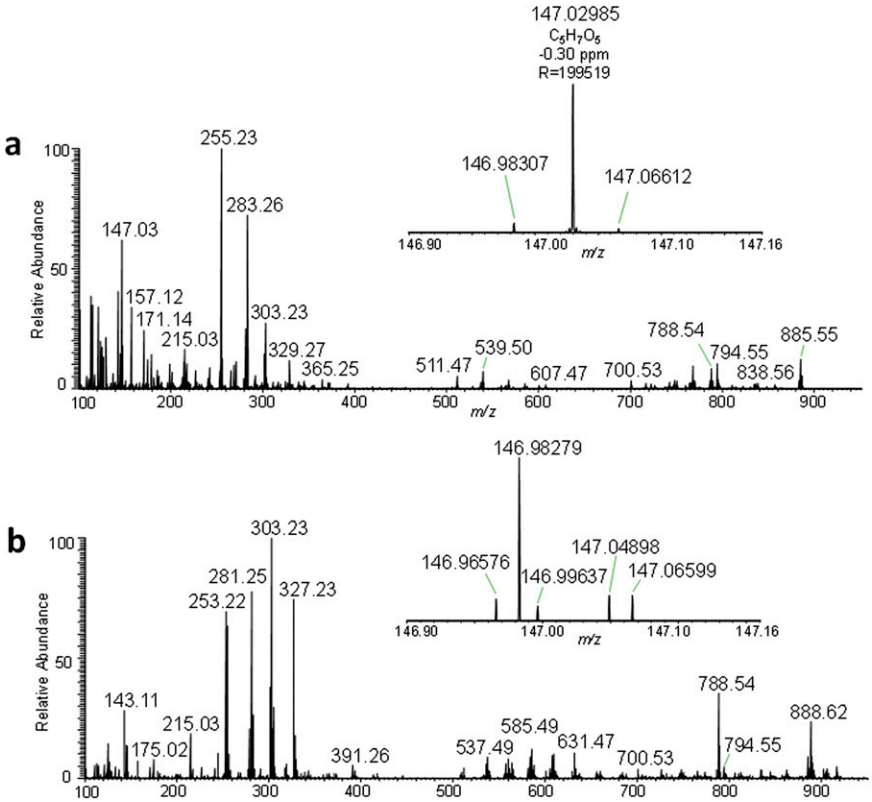

Fig. S3. Negative ion mode DESI mass spectra obtained in an LTQ Orbitrap mass spectrometer from *m/z* 100–1,000 for samples G42, an oligodendroglioma with the IDH1 R132H mutant with 2-HG signal at *m/z* 147.0299 (*A*) and G29 and a glioblastoma with wild-type IDH1 (*B*). (*Insets*) Zoomed-in region *m/z* 146.90–147.16.

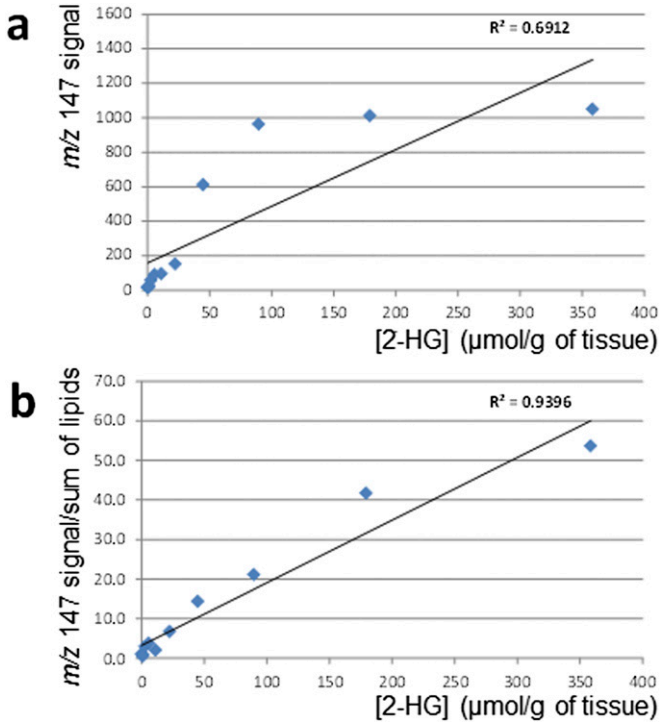

Fig. S4. Normalization of 2-HG signal and estimation of limit of detection. In DESI MS analysis, a tissue section of ~12 μm in thickness is examined on a pixel-by-pixel basis, with sampling area of 200 × 200 μm^2 for each mass spectrum acquired. An estimation of the total amount of 2-HG per pixel can be made by first estimating the mass of a 10- × 6-mm human brain tissue section of 12-μm thickness to be ~0.5 mg. The limit of detection of 2-HG was estimated by depositing different concentrations of standard 2-HG solutions onto mouse brain tissue, followed by DESI MS analysis under the same experimental conditions as for the human glioma samples analysis. (*A*) A correlation factor of (R^2 = 0.69) was determined when directly plotting the *m/z* 147 signal versus the known 2-HG concentration, (*B*) but a somewhat linear relationship was observed between the *m/z* 147 normalized to the sum of the 40 most abundant lipid species and the known 2-HG concentration (R^2 = 0.94) from the mouse brain tissue by DESI MSI. Note that the correlation in both plots is significantly improved if the concentration range is limited to 100 μmol/g. The limit of detection was estimated to be 3 μmol 2-HG/g of tissue.

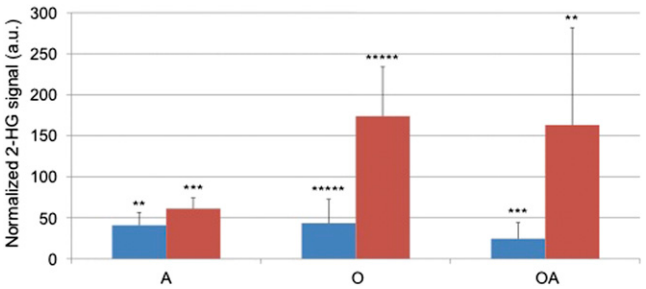

Fig. S5. Bar plot of normalized 2-HG signal versus tumor in a glioma series with IDH1 mutation (see Table 1 for sample details). Blue bars, low tumor cell concentration; red bars, high tumor cell concentration. A, astrocytomas; O, oligodendrogliomas; and OA, oligoastrocytomas.

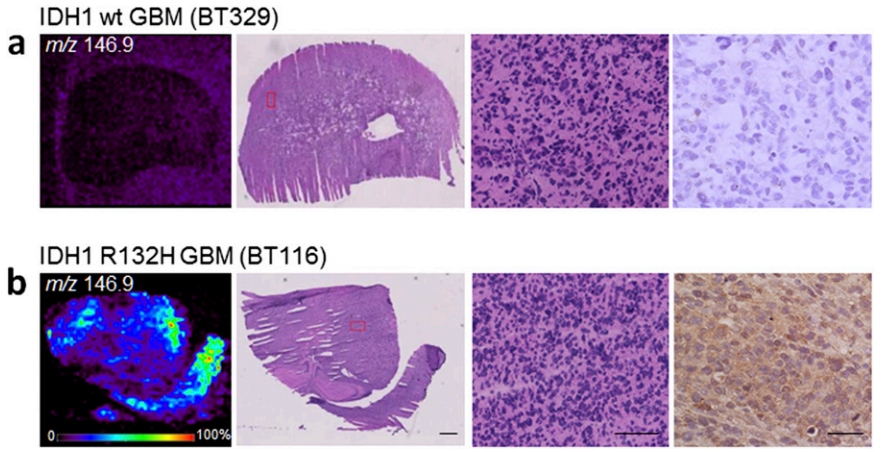

Fig. S6. Two-dimensional DESI MS ion images of human glioma cell xenografts in immunocompromised mice. (*A*) Negative ion mode 2D DESI MS images of human glioblastoma xenograft (BT329) that has wild-type IDH1 and (*B*) human glioblastoma xenograft (BT116) that has an IDH1 R132H mutation. The left panel is an ion map demonstrating the relative signal intensity of peak *m/z* 146.9, which was confirmed to be 2-HG by tandem MS analysis (MS^2 and MS^3). Relative signal intensity (0–100%) is plotted for each specimen using a color scale. Low magnification and high magnification light microscopy images of H&E-stained sections are shown, and IDH1 R132H point mutation specific antibody staining on the far-right panel. (Scale bar, 100 μm.)

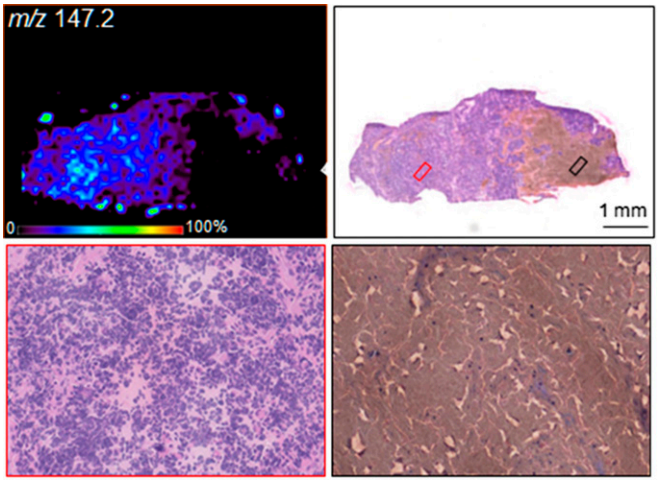

Fig. S7. Two-dimensional DESI MS ion images of human glioma resection specimen. Negative ion mode 2D DESI MS images from glioma resection specimens with IDH1 mutations. G30 (A-IV-O). (*Left*) An ion map demonstrating the relative signal intensity of peaks at *m/z* 146.7–147.2, which were each confirmed to be 2-HG by tandem MS analysis (MS^2). MS data for sample G30 was acquired using an LTQ ion trap (Thermo Fisher Scientific). Relative signal intensity (0–100%) is plotted for each specimen using a color scale. Low magnification light microscopy images of H&E-stained sections show the tissue outline. The red boxed area indicates a region of higher tumor cell concentration. The black boxed area indicates blood.

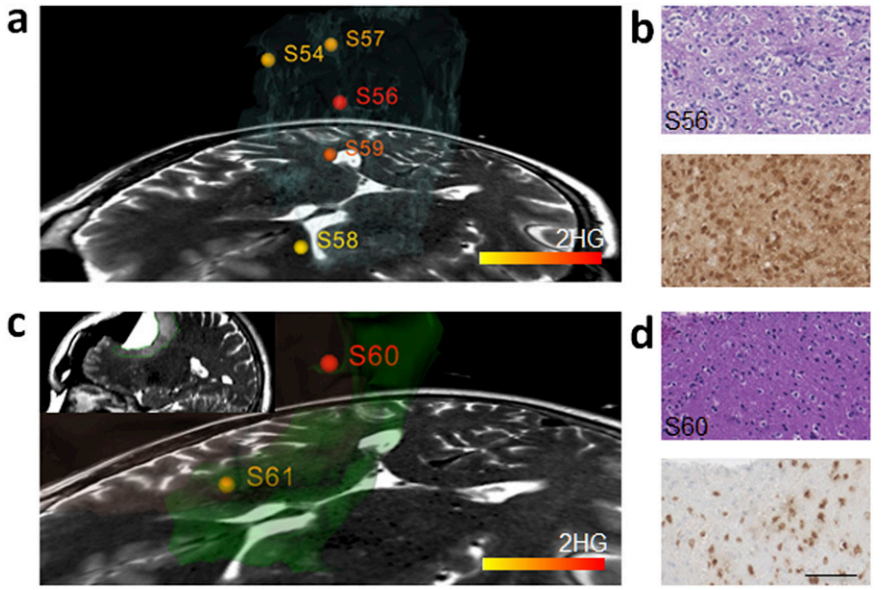

Fig. S8. Three-dimensional mapping of 2-HG over MRI volume reconstruction for surgical case 13, an oligoastrocytoma grade II. (*A*) Normalized 2-HG signal is represented with a warm color scale as indicated by the scale bar, set from the lowest to highest levels detected from this individual case. MS data were acquired on a DESI AmaZon Speed instrument. Stereotactic positions were digitally registered to the preoperative MRI using neuronavigation (BrainLab system) in the Advanced Multimodality Image Guided Operating (AMIGO) suite. (*B*) High magnification microscopy images of an H&E-stained section of FFPE tissue from sample S56 showing high tumor cell concentration (*Upper*) and of IHC for IDH1 R132H mutant (*Lower*). (*C*) 2-HG over tumor volume reconstruction from the T2-weighted intraoperative MRI. (*Inset*) The residual lesion. (*D*) High magnification microscopy images of H&E-stained sections of FFPE tissue from sample S60 showing the presence of residual tumor cells (*Upper*) and of IHC for IDH1 R132H mutant (*Lower*). (Scale bar, 100 μm.)

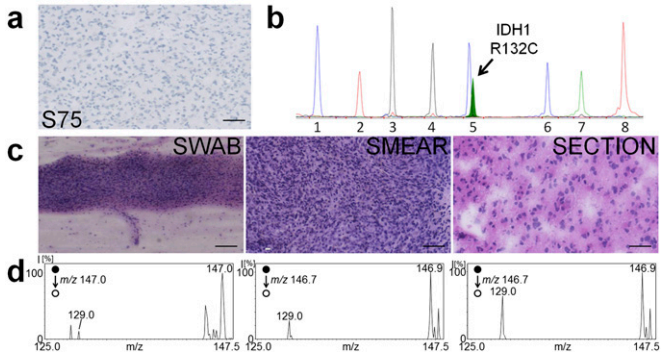

Fig. S9. (*A*) IHC using an IDH1 R132H point mutation-specific antibody on an FFPE section from oligoastrocytoma grade II samples (S75). (Scale bar, 100 μm.) (*B*) Targeted mutational profiling using SNaPshot analysis on nucleic acids extracted from oligoastrocytoma grade II archival specimens (S75). The arrow points to the IDH1 R132G (c.394C > G) mutant allele. The assayed loci were as follows: (1) KRAS 35, (2) EGFR 2236_50del R, (3) PTEN 517, (4) TP53 733, (5) IDH1 394, (6) PIK3CA 3139, (7) NOTCH1 4724, and (8) NOTCH1 4802. (C) High magnification light microscopy images of H&E-stained swab (*Left*), smear (*Center*), and frozen tissue section (*Right*) are shown. (Scale bar, 200 μm.) (*D*) Corresponding tandem mass spectra (MS^2) of *m/z* 147.0 (*Left*), 146.9 (*Center*), and 146.9 (*Right*) detected from sample S72 present a fragmentation pattern that exactly matches that of standard 2-HG.

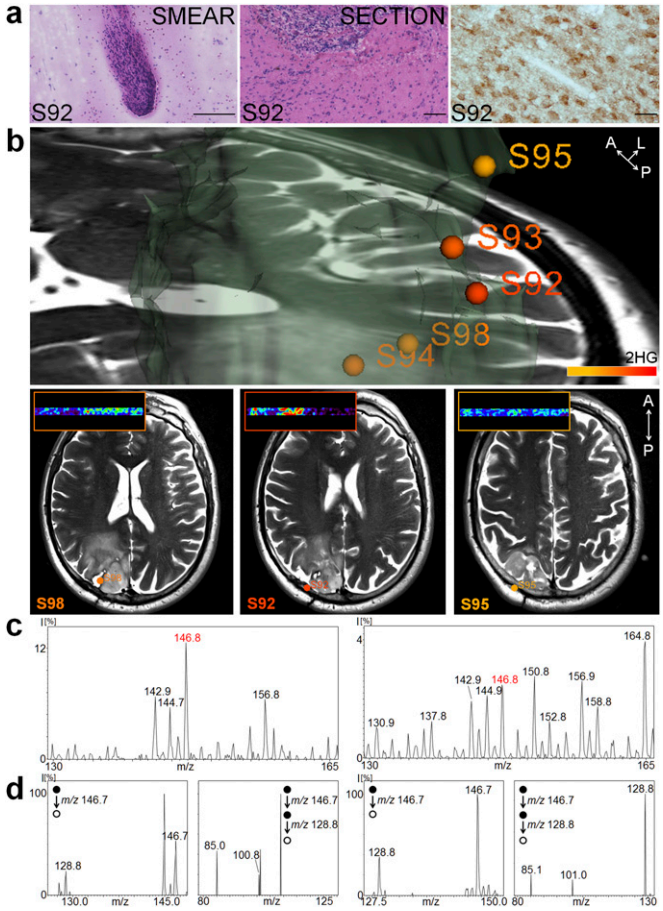

Fig. S10. (*A*) High magnification light microscopy images of H&E-stained smear (*Left*) and frozen tissue section (*Center*) of sample S92 are shown. (Scale bar, 200 μm.) IHC (*Right*) using an IDH1 R132H point mutation-specific antibody on an FFPE section from an oligoastrocytoma grade III sample (S92). (Scale bar, 20 μm.) (*B*) Normalized 2-HG signal for samples of case 28, an oligoastrocytoma grade III represented with a warm color scale as indicated by the scale bar, set from the lowest (yellow) to highest (red) levels detected from samples for this individual case. Stereotactic positions were digitally registered to the preoperative MRI using neuronavigation (BrainLab system) in a standard operating room. The 3D tumor volume is shown (*Upper*). Classification results of samples S98, S92, and S95 are further visualized on axial sections (*Lower*). (*Insets*) Negative ion mode 2D DESI MS images of 2-HG peak for smears of samples S98, S92, and S95. "Brain shift" after the craniotomy has resulted in sample S92's being mapped to the surface of the brain and S95 to just slightly outside of the brain. (*C*) Negative ion mode DESI mass spectra obtained using an amaZon Speed ion trap from *m/z* 130–165 (Bruker Daltonics) from a smear (*Left*) and a section (*Right*) for sample S92. (*D*) Corresponding tandem mass spectra (MS^2 and MS^3) of *m/z* 146.7 and 128.8 (smear, *Left*) and (section, *Right*) detected from sample S92 present a fragmentation pattern that exactly matches that of standard 2-HG.

Table S1. Detailed description of samples used in IDH1 study

Sample ID	Diagnosis	% tumor	IHC IDH1 R132H	Normalized *m/z* 147	2-HG
Low tumor cell concentration					
G10	O-II	30	Positive	12	Positive
G22	O-II	10	Positive	9	Positive
G25	O-II	20	Positive	72	Positive
G40	O-II	5	Positive	45	Positive
G13	OA-II	5	Positive	11	Positive
G14	OA-II	40	Positive	47	Positive
G9	O-II/III	50	Positive	44	Positive
G11	O-II/III	20	Positive	79	Positive
G20	OA-III	30	Positive	16	Positive
G26	A-IV	20	Positive	52	Positive
G47	A-IV-O	5	Positive	30	Positive
High tumor cell concentration					
G2	A-II	60	Positive	74	Positive
G49	O-II	100	Positive	87	Positive
G42	O-II	90	Positive	148	Positive
G43	O-II	80	Positive	241	Positive
G41	O-III	95	Positive	178	Positive
G23	O-III	95	Positive	215	Positive
G21	OA-III	95	Positive	247	Positive
G45	OA-III	100	Positive	79	Positive
G30	A-IV-O	80	Positive	48	Positive
G46	A-IV	90	ND	62	Positive
IDH wild type by IHC					
G3	A-III	60	Negative	10	Negative
G4	A-III	30	Negative	6	Negative
G5	A-IV-O	80	Negative	29	Negative
G6	A-IV	80	Negative	12	Negative
G8	A-IV	90	Negative	10	Negative
G27	A-IV	95	Negative	16	Negative
G28	A-IV	80	Negative	126	Positive
G29	A-IV-O	80	Negative	25	Negative
G31	A-IV	90	Negative	17	Negative
G32	A-IV	90	Negative	15	Negative
G33	A-IV	80	Negative	41	Positive
G34	A-IV	30	Negative	8	Negative
G35	A-IV	80	Negative	36	Negative
G48	A-IV	90	Negative	21	Negative

IHC and DESI results are shown. ND, not determined.